



UNICA

UNIVERSITÀ
DEGLI STUDI
DI CAGLIARI



Università di Cagliari

UNICA IRIS Institutional Research Information System

This is the Author's *accepted* manuscript version of the following contribution:

M. Petrollese, G. Concas, F. Lonis, D. Cocco, Techno-economic assessment of green hydrogen valley providing multiple end-users, International Journal of Hydrogen Energy, Vol. 47,2022, pp.24121-241355

The publisher's version is available at:

<http://dx.doi.org/10.1016/j.ijhydene.2022.04.210>

When citing, please refer to the published version.

© 2022. This manuscript version is made available under the CC-BY-NC-ND 4.0 license <https://creativecommons.org/licenses/by-nc-nd/4.0/>

This full text was downloaded from UNICA IRIS <https://iris.unica.it/>

Techno-economic assessment of green hydrogen valley providing multiple end-users

Mario Petrollese^{*}, Giulia Concas, Francesco Lonis, Daniele Cocco
Department of Mechanical Chemical and Material Engineering
University of Cagliari, Cagliari, Italy
e-mail: petrollese@unica.it

ABSTRACT

A techno-economic analysis of a hydrogen valley is carried out in this paper. A hydrogen generator fed by a wind farm (WF) and/or a photovoltaic (PV) plant supplies four end-users: a stationary fuel cell, a hydrogen refuelling station, the injection in the natural gas pipeline and, in case of sufficient hydrogen surplus, a biological hydrogen methanation – BHM process.

The results demonstrated that an efficiency improvement and a reduction of hydrogen production costs arise from a balanced supply from wind and solar energy. Without the inclusion of a BHM process, hydrogen production costs lower than 7 €/kg were achieved by a hydrogen generator using 10-12% of the PV+WF annual energy with a PV share of 20%-50%. The hydrogen production costs were further reduced to 5 €/kg by introducing a BHM process and increasing the percentage of electrical energy supplied by the PV+WF system to 25% of its the overall production.

KEYWORDS

Green hydrogen; hydrogen valley; RES curtailment; power-to-X; power-to-methane; biological hydrogen methanation.

^{*} Corresponding author

Nomenclature

Symbols

AC	operation and maintenance costs [€/year]
A	area [m ²]
EC	electricity purchasing costs [€/year]
f_{PV}	derating PV factor
i	annual interest rate
L	lifetime [years]
LCOH	Levelized Cost of Hydrogen [€/kg]
IC	initial costs [€]
\dot{m}	mass flow rate [kg/s]
$\dot{m}_{CH_4,out}$	CH ₄ output flow [Nm ³ /day]
$\dot{m}_{CH_4,in}$	CH ₄ input flow [Nm ³ /day]
n_{PV}	number of PV modules
n_{WT}	number of wind turbine
P	electrical power [kW]
T	temperature [°C]
V_r	biomethane reactor volume [m ³]
v	wind speed [m/s]
z	height [m]
ρ	density [kg/m ³]
η	efficiency

Acronyms

BHM	Biological Hydrogen Methanation
FCEV	Fuel Cell Electric Vehicles
O&M	Operation and maintenance costs
NG	Natural Gas
PEMEL	Polymeric Electrolyte Membrane Electrolyser
PPA	Power Purchase Agreement
PtG	Power-to-Gas
PtH	Power-to-Hydrogen
PV	Solar Photovoltaic
RES	Renewable Energy Sources
SOFC	Solide Oxide Fuel Cells
WF	Wind Farm

Subscripts

BL	Blending
EL	Electrolyser
RF	Refuelling station
ST	Hydrogen storage

1 INTRODUCTION

Power-to-X (PtX) technologies could play a fundamental role in the near future to support the penetration of renewable energy sources (RES) into the electricity supply mix by providing the required long-term storage capacity for non-dispatchable power generation units. Indeed, PtX technologies offer a realistic pathway to lower the greenhouse and polluting emissions of hard-to-abate sectors (in particular, transports and industry) through the exploitation of the energy surplus of RES power plants. Mainly, PtX technologies use electrical energy to produce hydrogen by means of water electrolysis processes (“Power-to-Hydrogen”, PtH). Hydrogen can be directly used as a fuel in the power generation, industrial, transport, and heating sectors or can be further converted to other energy carriers (methane, methanol etc.) [1]. For instance, methane can be produced from hydrogen along with carbon dioxide by using biological or thermochemical methanation processes (“Power-to-Methane”) [2]. To foster the substitution of fossil fuels with RES in the industrial, transport, and heating sectors, both hydrogen and methane could be injected into existing natural gas (NG) pipelines.

The advantages of PtH technologies are the capacity of storing large amounts of energy for long time [3], and providing a significant contribution to the development of intermittent RES power generation plants, such as solar photovoltaics (PV) or wind farms (WF). Moreover, the use of electrolysis systems coupled with RES, allows the production of highly pure H₂ with a low environmental impact [4]. Dedicated hydrogen strategies and roadmaps are being developed by the major world economies, including Japan, Germany, Australia and the European Union [5]. At the same time, different solutions for isolated hydrogen production systems from RES are studied and tested in different European countries [6]. Such isolated systems fall within the concept of “hydrogen valleys”, which are based on a combination of several hydrogen technologies into an integrated hydrogen ecosystem (a city, a region, an island, or an industrial district). A hydrogen valley should ideally cover the entire hydrogen value chain: production, storage, distribution, and final use. The growing interest in the use of hydrogen as energy carrier and in the “Power-to-Hydrogen” concept is proved by many European projects involving different hydrogen technologies. In this regard, HyStock [7], the first power-to-gas (PtG) system in the Netherlands, is a project developed by EnergyStock and based on a 1 MW polymeric electrolyte membrane electrolyser (PEMEL) partially fed by a 1 MW PV solar field. The hydrogen is stored in pressurised tanks and transported to the end-users. The project aims to investigate the benefits of the PEMEL to provide ancillary services for the power grid. HyBalance [8] is a Danish PtH system that exploits the excess wind power to produce hydrogen and balance the grid demand. The hydrogen is then used in the transport and industrial sectors. H2Future [9] is a project proposed by the Voestalpine Linz steel production site in Austria and based on a 6 MW electrolyser. The project aims to study the use of electrolysers to provide grid balancing services such as primary, secondary, and tertiary reserves, while also providing hydrogen to the steel plant. The hydrogen would be produced by using electricity generated during off-peak hours to take advantage of time-of-use power prices. The REFHYNE project [10], in Germany, consists of a 10 MW electrolyser established at a large oil refinery in Rhineland to provide the hydrogen required for refinery processes. The electrolyser is expected to replace the existing H₂ supply facility based on two steam methane reformers. At the same time, the electrolyser is expected to balance the internal electrical grid of the refinery and to provide primary control reserve services to German transmission system operators. The GRHYD [11] project in France aims to convert the surplus energy generated from RES into H₂. The hydrogen is blended with natural gas and injected into the existing pipeline. The project aims to demonstrate the technical, economic, environmental, and social advantages of mixing hydrogen with NG as a sustainable energy solution [12]. The potential of PtX technologies is therefore of great importance, especially for local districts characterised by the presence of RES power generation plants and different energy users. For example, the project “Renewislands -

Renewable Energy Solutions for Islands” integrates intermittent renewable energy supply, fuel cells, and hydrogen production for decentralised power systems penetration [13].

The synergy between RES plants, electrolysis systems, and green fuels production is also deeply discussed in literature (an overview of different Power-to-Hydrogen studies for a comparative evaluation is given in [14]). Kotowicz et al. [15] investigated three different possibilities of cooperation between a WF and an alkaline electrolyser. The work aimed to match the rated power of the wind farm with that of the H₂ generator to reach the highest system efficiency. Cheli et al. [16] presented a steady-state analysis of a local natural gas distribution network used as RES energy surplus storage in form of H₂ blending. The objective was to recreate a small and simplified urban gas network integrated with a PtG system and to discuss the blending quantities and effect. Peyerl et al. [17] developed an economic analysis of a renewable hybrid system for H₂ production and storage. Results demonstrated that implementing a wind farm and a PV plant to include renewable H₂ in the power sector can be profitable only if the H₂ is used as fuel and not converted back into power. Kim et al. [18] analyzed different process models to compare the economic, environmental, and social performance of the H₂ supply using wind power and natural gas. Results demonstrated the benefits in terms of reduction of CO₂ emission and customer satisfaction while from an economical point of view, producing H₂ using natural gas remains the most profitable scenario. Liu et al. [2] employed an optimal operational model to develop a hybrid power-natural gas energy system. Power-to-Hydrogen and Power-to-Methane technologies were included in the energy system and compared to show the benefits of the reduced curtailment of wind power, the reduction of operational costs, and the decline of CO₂ emissions. Fang et. al [19] proposed a life-cycle economic assessment of a wind power-H₂ coupled integrated energy system. The results showed a short payback period and high cumulative return. Nastasi and Lo Basso [20] carried out an analysis on the potential of the PtG concept within the Power-to-Heat strategy applied to a city considering three reference cases under different urban energy scenarios based on different RES shares. Even though the PtG concept could play an important role in the decarbonisation of island contexts, the low efficiencies and high costs related to the hydrogen generation should be kept in mind [21,22].

All the above papers demonstrated that the optimal design of a hydrogen valley is not univocal, but it depends on penetration and nature of RES systems, final use of the hydrogen and end-users’ requests, objective function chosen and so on. Therefore, further investigations are demanded to propose effective methods for identifying the best hydrogen valley configuration in terms of optimal ratio between hydrogen generators size and RES-based nominal power, storage capacity and best mix among RES generators, especially if the hydrogen is required by different end users. In this framework, a preliminary techno-economic analysis for the development of a hydrogen valley is carried out in this study. Starting from the availability of a given share of the yearly energy production of a wind farm and/or a photovoltaic power plant, the expected annual performance of a green hydrogen system based on a PEMEL, and a hydrogen storage section is analysed. The hydrogen can be used by different end-users, such as a stationary fuel cell power system, a hydrogen refuelling station, the blending in a NG pipeline, and a biomethanation process. Different sizes for both the PEMEL and the H₂ storage section are considered and analysed as well as different percentage of the electrical energy supplied by the wind farm and the photovoltaic system. A preliminary economic analysis is then carried out to assess the most suitable system configuration, in terms of PEMEL rated power, hydrogen storage capacity and WF/PV mix supply able to reach the minimum hydrogen production cost. Because of the insularity, the availability of many RES power plants (exceeding 2 GW) and the strong seasonality of the energy demand, the development of a hydrogen valley in the industrial area of Cagliari (Sardinia, Italy) is considered as case study. The original contribution of this paper is therefore:

- the investigation of the best configuration of a green hydrogen supply chain (electrical generators based on different RES, hydrogen generator size, hydrogen storage capacity) designed to satisfy different end-user demands
- to evaluate the feasibility and profitability of coupling the hydrogen valley with a biomethanation process in terms of reduction of the hydrogen production costs.

2 SYSTEM CONFIGURATION

The energy system analysed in this work employs the electrical energy surplus of a wind farm (WF) and/or a photovoltaic (PV) plant and, in case, green energy supplied by the electrical grid to produce hydrogen for different end-users, in particular: a refuelling station for fuel cell electric vehicles (FCEV), a stationary fuel cell, the injection in the district NG pipeline, and the production of biomethane to be injected in the same NG pipeline. Figure 1 shows the conceptual scheme of the proposed hydrogen valley.

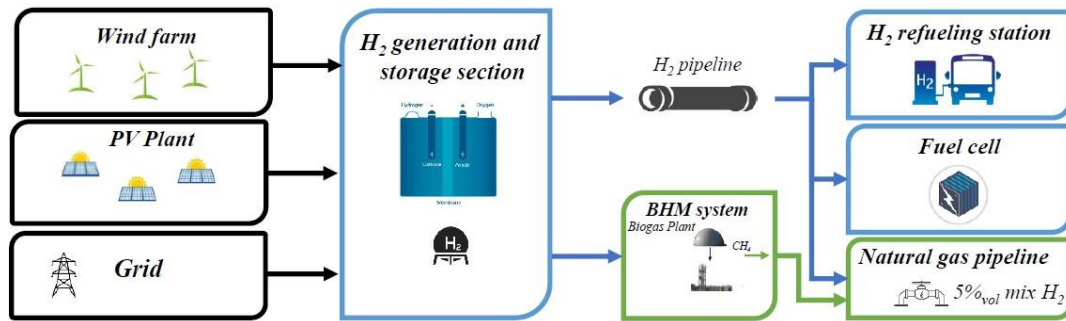


Figure 1. Conceptual scheme of the hydrogen valley.

As a reference case, the hydrogen valley consists of a MW-scale PEMEL unit fed by a share of the electrical energy produced by an existing 45 MW wind farm without considering any support from the photovoltaic plant. In case wind power is not available, the electrolyser can be fed by electricity from the grid. By means of a proper Power Purchase Agreement (PPA) with a Third-party commercial supplier, this further energy demand could be covered by other RES plants located near the hydrogen valley, assuring the production of 100% green hydrogen. Obviously, the cost of the energy purchased from the grid will be much higher than the cost of the energy supplied by the dedicated RES power plants as it includes not only production costs but also service charges, dispatching costs, taxes, etc. The hydrogen generation system is designed to use a given percentage of the wind farm rated power. Moreover, during operating periods, the wind farm supplies the same percentage of its hourly electrical energy production to the PEMEL for hydrogen production. Since a mismatch between hydrogen supply and demand is expected, the hydrogen valley is also equipped with a H₂ storage section with an operating pressure range of 2-30 bar. The influence of both PEMEL size and H₂ storage capacity on the performance of the overall system is analysed in this study. The H₂ is injected in a special hydrogen pipeline, to feed in order: a fleet of FCEV (such as buses, last-mile logistics, and a train) and a stationary fuel cell to provide electricity to the train and bus station, while the remainder H₂ is injected in the district NG pipeline considering a maximum safety limit of 5%_{vol}. When the safety limit of the NG grid is reached and all the hydrogen demands are satisfied, the eventual H₂ overproduction can be used to synthesise biomethane suitable for the injection in the NG grid. For this purpose, a biological hydrogen methanation (BHM) process is considered to convert all the CO₂ produced by the biogas upgrading section of an anaerobic digestion plant. Two different cases are analysed to ensure the continuous operation of the BHM

reactor. The first methanation system includes an auxiliary PEMEL, the second, an auxiliary PEMEL along with an additional H₂ storage tank.

Finally, the electrical energy surplus of a photovoltaic plant characterized by the same nominal power of the wind farm is also considered in addition or in alternative to the wind farm. As known, the capacity factor of the PV plant is lower than the WF one, but its daily production profile is more regular and a better matching between hydrogen production and end-user demand may occur. The effect of a complete or a partial substitution of the electrical energy produced by the WF with that produced by the photovoltaic system on the main performance results is therefore investigated in this paper.

3 METHODS

The yearly performance of the hydrogen valley was evaluated by means of specific mathematical models developed in MATLAB and Aspen Plus environments. As case study, it was assumed that the hydrogen valley is sited in the industrial area of Cagliari (Italy) near to an existing wind farm. Meteorological data for the considered location were determined by Meteonorm software [23]. A rule-based operating strategy was implemented for managing the hydrogen storage section and the expected energy and mass flows of the hydrogen valley were determined on hourly based analysis. A parametric analysis is therefore carried out by varying the size of the hydrogen generator, the hydrogen storage capacity and the share of the PV rated power compared to the WF one. The expected hydrogen production costs are then calculated by means of a preliminary economic analysis.

3.1 Wind farm

The wind farm considered for the electrical supply of the hydrogen generators consists of 30 wind turbines with a total rated power of 45 MW. Table 1 reports the main wind farm characteristics. Meteorological data, particularly wind speed at a height of 10 m above the ground (v_{10}), were determined by Meteonorm software for each hour of a typical year. Wind speed at the hub height (v_{hub}) was calculated following equation (1), where α is the wind shear exponent, chosen equal to 0.25 within a typical range of 0.1-0.4 [24]:

$$v_{hub} = v_{10} \left(\frac{z_{hub}}{z_{10}} \right)^\alpha \quad (1)$$

The wind speed frequency distribution was calculated by considering 27 wind classes with an amplitude of 1 m/s. The wind distribution (in hours/year) is shown in Figure 2(a). The figure also shows the power curve of the considered wind turbine (with reference to a standard density of 1.225 kg/m³) [25].

Table 1. Wind turbines and wind farm parameters [25].

Parameter	Value
Wind turbine rated power	1.5 MW
Hub height (z_{hub})	80 m
Rotor diameter	77 m
Cut-in wind speed	3 m/s
Rated wind speed	11.1 m/s
Cut-out wind speed	25 m/s
Auxiliary consumption (P_{aux})	2%
Wake losses (k_w)	5%

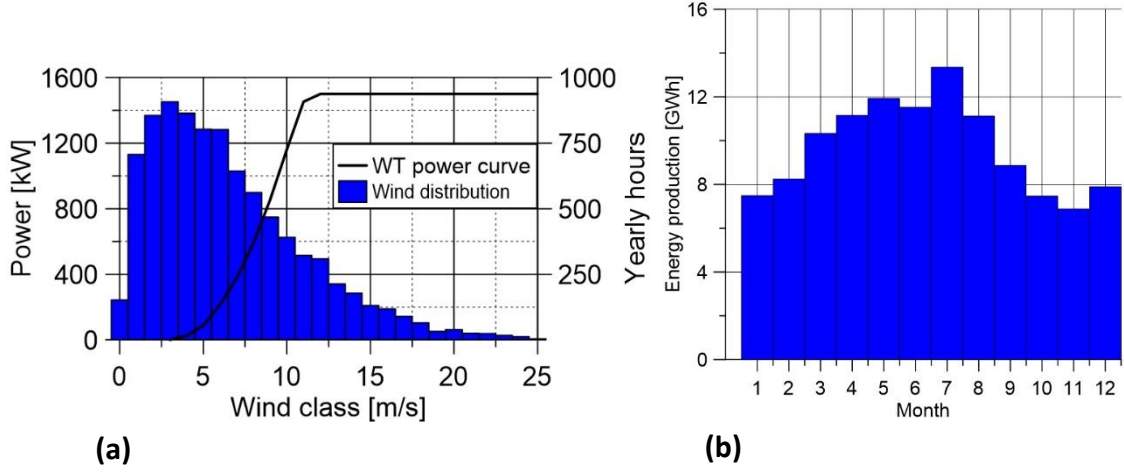


Figure 2 (a) Wind turbine power curve (left y-axis) and wind frequency distribution (right y-axis); (b) expected monthly energy production.

The hourly power production of the wind farm (P_{WF}) is evaluated by considering the effect of actual air density (ρ/ρ_0 , calculated as a function of hourly temperature and pressure by assuming air as ideal gas), wake losses (k_w), and auxiliary consumption (P_{aux}).

$$P_{WF} = n_{WT} P_{WT} (\rho/\rho_0) (1 - P_{aux}) (1 - k_w) \quad (2)$$

where n_{WT} is the number of wind turbines (30) and P_{WT} is the power produced by the single wind turbine calculated according to the wind speed at the hub height and the corresponding power curve. The annual energy production of the wind plant, calculated as the sum of the wind farm hourly energy production, is about 116 GWh/year while Figure 2(b) shows the monthly energy production.

3.2 Photovoltaic system

A photovoltaic system with a rated power output equal to that of the wind farm is considered as an alternative energy supplier of the hydrogen generation system.

A 360 Wp PV panel with a tilt angle equal to 30° and oriented toward south was considered for the simulation of the annual performance of the solar power plant. The other main PV panel characteristics are reported in Table 2.

Starting from the hourly solar irradiation GI available on the surface of the PV array given by Meteonorm (Figure 3 (a)), the conversion efficiency of the PV module (η_{PV}) is determined by the following correlation:

$$\eta_{PV} = \eta_{PV,STC} [1 + \gamma (T_{CELL} - 25^\circ C)] \quad (3)$$

where $\eta_{PV,STC}$ is the PV efficiency under standard test conditions (STC), γ is the temperature coefficient and T_{CELL} is the and calculated.

The hourly power output of the photovoltaic plant is therefore calculated as:

$$P_{PV} = n_{PV} A_{PV} GI \eta_{PV} \eta_{INV} f_{PV} \quad (4)$$

where n_{PV} is the overall number of PV modules A_{PV} is the active panel area, η_{INV} is the inverter efficiency, while f_{PV} is a derating factor representative of secondary losses such as soiling loss, wiring losses, aging etc. The number of PV modules is set to 142000, to obtain a peak power of the PV array of about 51 MW corresponding to a nominal AC power of 45 MW, equal to the rated power of the wind farm. The calculated annual energy production of the photovoltaic plant is about 80 GWh/year, Figure 3 (b) shows the monthly energy production.

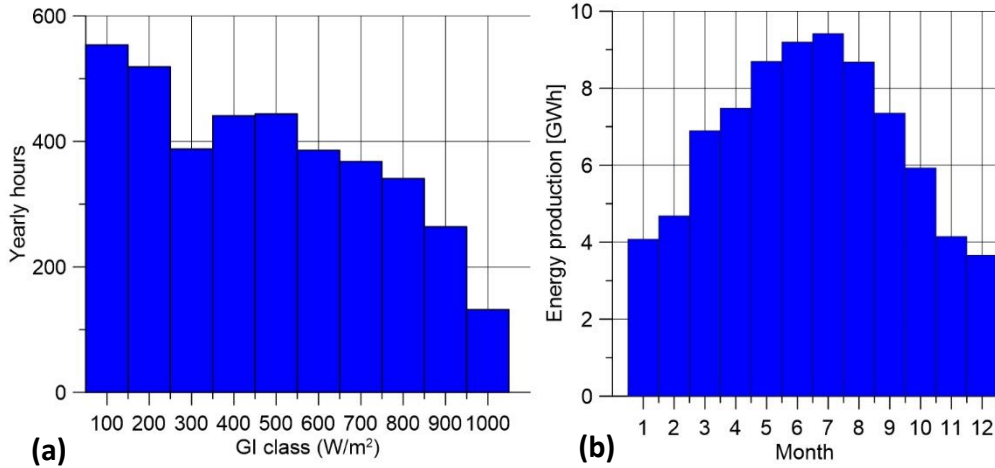


Figure 3. (a) global solar irradiation available on the surface of the PV array and (b) monthly energy production.

Table 2. Photovoltaic system parameters [27].

Parameter	Value
PV peak power	360 W
PV Net operative cell temperature (T_{NOCT})	41.5°C
PV efficiency under STC ($\eta_{PV,STC}$)	22.1%
Active panel area (A_{PV})	1.630 m ²
PV temperature coefficient (γ)	-0.29%/K
Derating factor (f_{PV})	0.9
Inverter efficiency (η_{INV})	97%

3.3 Hydrogen generation system

Since the operation of the H₂ production unit is based on variable power generation profile due to the intermittent nature of wind and solar sources, a polymeric membrane electrolyser (PEMEL) was chosen. Among the three available water electrolysis technologies (i.e., alkaline, PEM, and solid oxide), PEMEL technology is the most suitable for following a RES load. PEMEL is particularly suitable for transient operation due to its ability to operate from 0 to 160% of its nominal load, with start-up times from 1 second to 5 minutes, a shutdown time in the order of seconds and, most importantly, a ramping speed of 100%/s (i.e., a system response in the order of few milliseconds) [28,29]. These features allow PEMEL to perform an instant load following of RES power profiles.

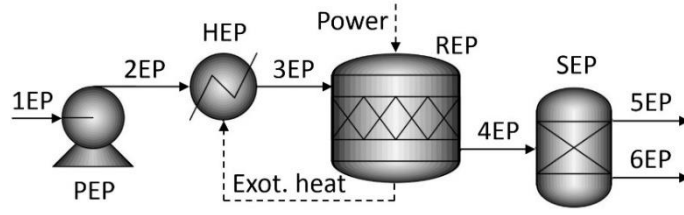


Figure 4. Simplified flowsheet diagram of the PEMEL.

The most common operating temperature of PEMEL is between 50 and 80 °C [30], while the operating pressure can be as high as 200 bar [29]. Typical lifetime of commercial stacks is in the range from 20,000 to 60,000 h [29].

To simulate the water electrolysis process, a specific model was developed in Aspen Plus adapting an electrochemical model developed and validated by Zhao and Brouwer [31,32]. Figure 4 shows the simplified Aspen model developed for the simulation of the PEMEL unit.

The water entering the electrolysis section is pumped to the operating pressure (30 bar) of the electrolyser by a pump (PEP) and heated to the operating temperature (80°C) by recovering the heat produced by the same electrochemical process (simulated with a heater block, HEP). The water splitting reaction ($H_2O \rightarrow H_2 + \frac{1}{2}O_2$) is carried out in an RStoic reactor (REP) with a conversion ratio of 1. Then, hydrogen (5EP) and oxygen (6EP), that due to the nature of the simulation leave the reactor as mixed species (4EP), are split by a separator (SEP).

The electrochemical model was based on a PEMEL stack composed of 20 cells in series, with a rated stack current of 135 A, a rated stack voltage of 48 V, and a nominal power of 6.5 kW [31,32]. In addition, an AC/DC conversion efficiency equal to 0.97 was considered. Finally, the consumption of pumps and auxiliaries was considered to calculate the total power absorbed by the PEMEL system. Table 3 summarises the technical characteristics of the PEMEL.

Table 3. PEMEL technical characteristics.

Parameter	Value
Number of cells	20
Rated stack current	135 A
Rated stack voltage	48 V
Nominal stack power	6.5 kW
Nominal PEMEL power	6.64 kW

The developed PEMEL model is therefore used for calculating the produced hydrogen mass flow rate (\dot{m}_{H_2}) in function of the electrical power input (P_{EL}) and the consequent PEMEL efficiency, expressed as:

$$\eta_{EL} = \frac{\dot{m}_{H_2} LHV_{H_2}}{P_{EL}} \quad (5)$$

where LHV_{H_2} is the hydrogen lower heating value (120 MJ/kg). Figure 5 shows the hydrogen mass flow production (a) and the net conversion efficiency (b) as a function of the stack power. As expected, the hydrogen production increases with the rise of the stack power. However, as well known the conversion efficiency decreases with the rise in the stack power (and, thus, in the current density) due to the prevailing role of ohmic losses, which increase almost linearly with the current density, while the activation losses are responsible of the significant performance reduction observed at low stack power [33]. The required size of the electrolyser was achieved by varying the total number of 20-cell stacks composing the PEMEL unit.

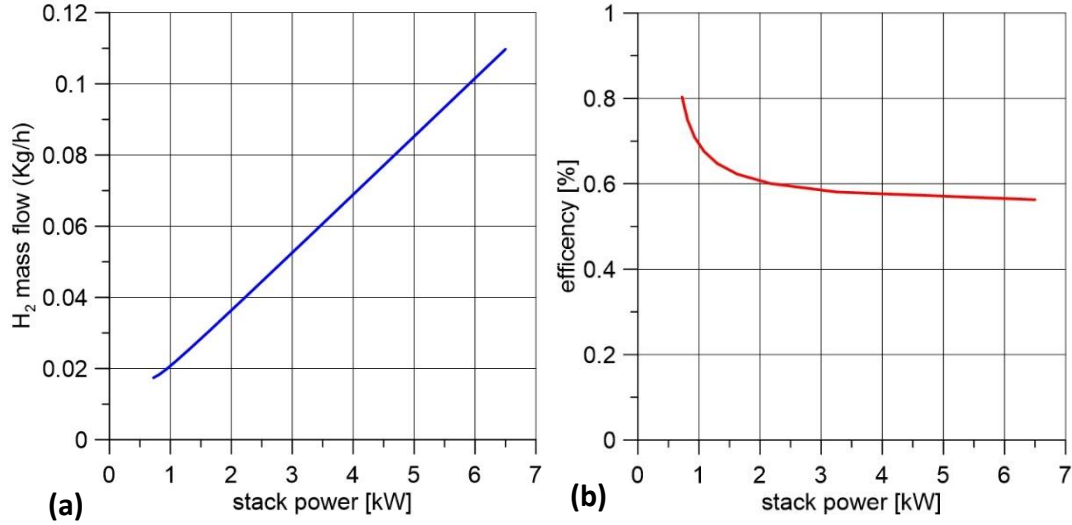


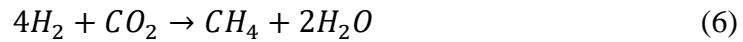
Figure 5. Hydrogen production (a) and net efficiency (b) as a function of the stack power.

3.4 Hydrogen demand

As mentioned, the hydrogen valley includes four hydrogen end-users: a stationary power generation unit, a hydrogen refuelling station, the injection on the NG pipeline, and the production of biomethane. The hydrogen demand is characterized by considering existing end-users of the industrial district potentially interested to the inclusion in the hydrogen valley. In detail, a solid oxide fuel cell (SOFC) unit characterised by a nominal power of 400 kW_e is considered to partially cover the heat and electricity demand of a railway station hub. Based on typical electrical and thermal loads, the SOFC operates from 8 a.m. to 8 p.m. every day under nominal conditions, for an annual electrical energy production of about 1.75 GWh/year. An expected hydrogen demand of 90 t/year (the corresponding SOFC specific consumption is therefore 51.4 kg/kWh [34]) is therefore assumed for this hydrogen end-user. The hydrogen refuelling station is designed to serve a fleet of 6 FC buses with a daily mileage of 200 km/day. By assuming an average specific consumption of 0.15 kg/km, the refuelling station should provide 180 kg/day of H₂, with an annual hydrogen consumption of 65.7 t/year. The refuelling station is equipped with a compression system to increase the hydrogen pressure up to 500 bar (it is assumed that the energy consumption of the compressors is in charge to the owner of the refuelling station and therefore it was not included in the energy balance of the hydrogen valley) and with a storage tank with a capacity of about 200 kg. The refuelling of the 6 FC buses occurs every day at 7 a.m., with a completely discharge of the refuelling station storage tank. The latter is then charged during the day, when the hydrogen produced by the PEMEL exceeds the SOFC demand. In case the tank is not completely charged at 3 a.m. of the following day, a constant hydrogen demand, either produced by electrical energy supplied by the WF, the PV or by the grid, is required for four hours up to reach the complete charging of the tank. Together with these two direct hydrogen consumptions, the coupling of the hydrogen valley with the NG pipeline of the industrial district is considered. In particular, the injection of 0-5%_{vol} of hydrogen in the NG pipeline, characterised by an expected NG consumption of 30 Mm³_{NG}/year, is introduced as a first option. This variable percentage of blending allows smoothing the fluctuations of the renewable hydrogen generation and reduces the CO₂ emissions by

substituting a portion of the fossil NG with green H₂. The hourly percentage of hydrogen injection is calculated to compensate the difference between the expected annual hydrogen production and the hydrogen demand of both the SOFC and refuelling station. However, the blending is limited to 5%_{vol} due to technological limits and to avoid large variations in the lower heating value of the NG. Consequently, the maximum amount of hydrogen injected in the NG grid is about 133 t/year.

Furthermore, if the annual hydrogen production surplus (amount of produced H₂ neither used in the SOFC and refuelling station nor injected in the NG pipeline), exceeds a given amount (180 t/year in this case), a methanation process is introduced as a further end-user in the hydrogen valley. As mentioned, two different BHM systems are considered. In the first solution, the biomethane reactor is introduced to exploit a constant hydrogen demand of about 155 kg/h, which is equal to the maximum H₂ production peaking. In the second, the bioreactor operated with a hydrogen capacity equal to 77 kg/h, representing half of the maximum hourly surplus value. The methanation process can be based on the chemical or biological conversion of carbon dioxide and hydrogen into methane and water, according to the Sabatier reaction (6):



The methane yield of the process strongly depends on the operating pressure and temperature. The catalytic methanation process is typically carried out at temperatures between 200 and 550 °C and pressures ranging from 1 to 100 bar, depending on the catalyst used. In the biological methanation, autotrophic hydrogenotrophic methanogens play the role of an autocatalyst and the operating temperature and pressure depend on their range of activity (0-122 °C, 1-10 bar). Nevertheless, the most common operating conditions for these systems are 20–70 °C and 1 bar [12]. Biological process has a reaction rate lower than chemical methanation due to a lower operating temperature. On the other hand, BHM has a high tolerance to impurities of the incoming gas and a simple process setup [35]. Another advantage of the BHM is its synergy with conventional anaerobic digestion processes [36]. Thus, an ex-situ BHM process was considered in this work. The BHM process model was developed in MATLAB and the specific calculation code is based on the performance of the ex-situ reactor of an experimental configuration [37]. Table 4 summarises the main parameters of the process. The most important design parameter is the Methane Formation Rate (MFR (Nm³/d)/m³) (7). It is defined as the difference between the CH₄ output and input flows (the latter is greater than zero if the injected gas is biogas), related to the reactor volume. The required CO₂ has been here assumed as recovered by an upgrading process from an anaerobic digestion plant, assuming a biogas composition of 45%_{vol} of CO₂ and 54%_{vol} of CH₄. If the produced biogas in the methanation reactor matches the requirements of the natural gas grid, it is commonly called "biomethane" and can be injected directly into the NG grid [36].

$$MFR = \frac{\dot{m}_{CH_4,out} - \dot{m}_{CH_4,in}}{V_r} \quad (7)$$

Table 4. BHM process parameters.

Parameter	Value
Retention Time (RT)	24 h
Methane Formation Rate (MFR)	3.7 (Nm ³ /d)/m ³
%H _{2,in}	80
%CO _{2,in}	20
%CH _{4,out}	96
%CO _{2,out}	4
%H _{2,out}	0

3.5 Hydrogen storage

Since both the electrical energy produced by the WF/PV and the hydrogen demand are variable over time, a mismatch between H₂ generation and request usually occurs. The H₂ pipeline, used to connect all the components of the hydrogen valley and characterised by an inner diameter of 0.1 m and an overall length of 5 km, can operate as a first storage system. By considering a maximum pressure of 30 bar (the delivery pressure of the PEMEL) and a minimum pressure of 2 bar (the pressure required by the SOFC), the hydrogen pipeline offers a storage capacity of about 90 kg of H₂. Consequently, the pipeline can face only a small share of the mismatch between production and demand of hydrogen. Therefore, the full exploitation of the hydrogen valley potentiality requires the introduction of larger storage capacities. For this reason, the hydrogen valley can include a dedicated storage section located near the PEMEL unit and with an operating pressure range of 2-30 bar. The operating strategy adopted for the management of the hydrogen storage on an hourly basis is shown in Figure 6. Firstly, the expected hydrogen production with the sole WF/PV supply (\dot{m}_{WF+PV}) is compared with the overall hydrogen demand given by the SOFC (\dot{m}_{SOFC}), the refuelling station (\dot{m}_{RF}) and the blending at the nominal allowable percentage ($\dot{m}_{BL,nom}$). In case of deficit in the hydrogen supply, the latter is covered by the hydrogen stored in the dedicated storage section and vice versa, the eventual surplus in the hydrogen production is stored for a postponed use.

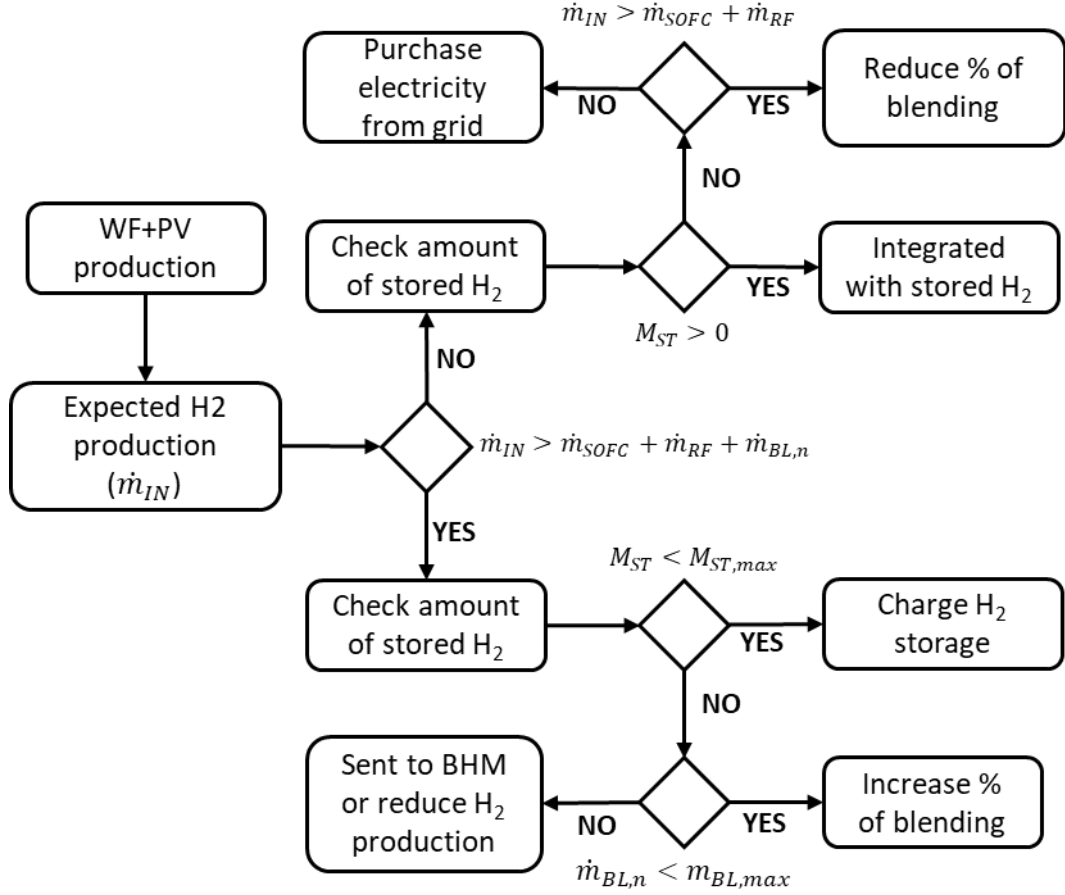


Figure 6 – Operating strategy for the management of the hydrogen storage section.

However, the tank capacity is limited and often unable to deal with the variability of the WF/PV energy production. In case the storage section is completely empty ($M_{ST} = 0$), the hydrogen management strategy provides to firstly reduce the percentage of hydrogen injected in the NG grid down to zero. If a gap in the hydrogen supply still occurs, the electrolyser is fed by electrical energy supplied by the grid. On the contrary, if the storage section is fully charged ($M_{ST} = M_{ST,max}$), the eventual surplus in hydrogen production is used to increase the blending up to 5%. If this increase is not enough, the production of hydrogen is reduced or, if present, it is sent to the BHM process. The proposed operating strategy is therefore developed to satisfy both the electrical energy balance and the hydrogen mass balance:

$$P_{WF} + P_{PV} + P_{GRID,IN} = P_{EL} - P_{GRID,OUT} \quad (8)$$

$$\dot{m}_{IN} + \dot{m}_{ST,D} = \dot{m}_{SOFC} + \dot{m}_{RF} + \dot{m}_{BL} + \dot{m}_{BHM} + \dot{m}_{ST,C} \quad (9)$$

where $P_{GRID,IN}$ and $P_{GRID,OUT}$ are the electrical power purchased and sold to the grid respectively, while $\dot{m}_{ST,C}$ and $\dot{m}_{ST,D}$ are the inlet/ outlet hydrogen mass flow to/from the hydrogen storage section, respectively. It is worth noting that for satisfying the hydrogen mass balance, a variation in the daily hydrogen demand profile occurs. By way of example, Figure 7 shows the daily hydrogen profile for two typical days. On the right, the hydrogen demand during a windy and sunny day where a large amount of green hydrogen is produced. In this case, the hydrogen can completely satisfy the demand of the SOFC, the refuelling station, the blending at its maximum percentage as well as a share of the hydrogen demanded by the BHM. On the contrary, only the SOFC and refuelling station request can be satisfied in the case shown

on the left, while the blending is not continuously guaranteed, and no contribution is given to the BHM process.

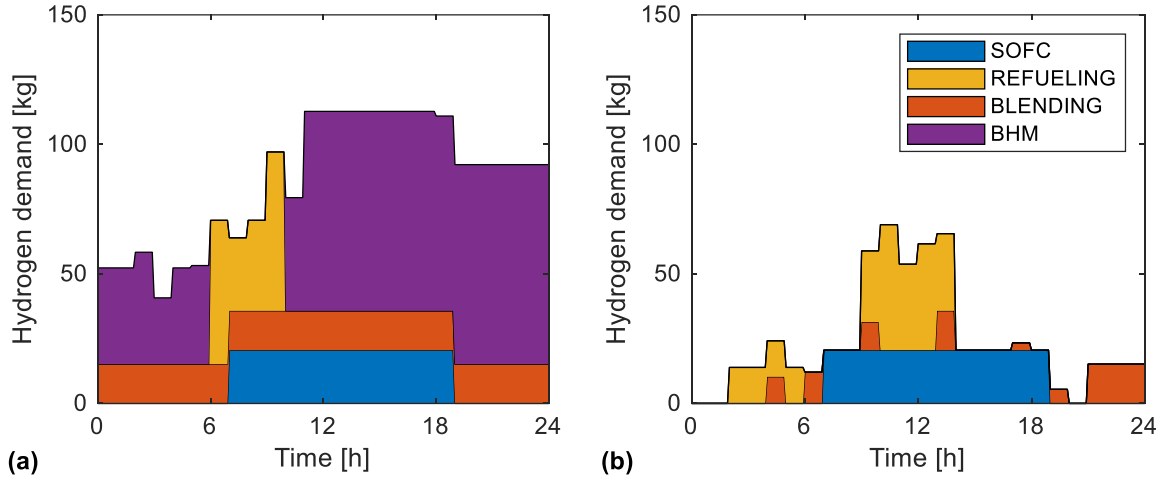


Figure 7 – Hydrogen daily demand during (a) periods with large hydrogen production and (b) periods with low hydrogen production.

3.6 Preliminary economic analysis

A preliminary economic analysis was carried out to investigate the cost-effectiveness of the proposed hydrogen valley and the optimal design from an economic perspective. The analysis considers the levelized cost of hydrogen (LCOH) as the main economic index:

$$\text{LCOH} = \frac{\text{IC} + \sum_{k=1}^L (\text{AC}_k + \text{EC}_k + \text{RC}_k) \cdot (1 + i)^{-k}}{\sum_{k=1}^L m_{\text{H}_2,k} \cdot (1 + i)^{-k}} \quad (10)$$

where IC are the investment costs incurred at the beginning of the lifetime; AC are the annual costs due to operation and maintenance, EC are the electricity purchasing cost, RC are the replacement costs, m_{H_2} is the annual hydrogen production, i is the annual interest rate, and L is the hydrogen valley lifetime. IC includes the direct electrolyser costs (stack and balance of plant), direct tank volume costs, and overall indirect costs (site preparation costs, contingency costs, engineering costs). Annual operating and maintenance costs, electricity purchasing costs and yearly hydrogen production were considered constant during the lifetime. Electricity costs are calculated by considering the different share of electricity coming from WF, PV and grid and by assuming for WF and PV the levelized electricity costs published by IRENA for Italy [38]. A typical market price is considered for the electricity purchased from the grid. Finally, replacement costs (50% of the direct electrolyser costs) are due the substitution of the stack after 50000 hours of the operation. Table 5 reports the main assumptions for the preliminary economic analysis.

Table 5. Main assumptions for the economic analysis.

Cost item	Value/Correlation	Ref
Electrolyser specific direct costs	$1160 \frac{\text{€}}{\text{kW}} \left(\frac{P_{\text{EL}}}{1000 \text{ kW}} \right)^{-0.2}$	[39]
Electrolyser specific indirect costs	$25\% c_{\text{EL,D}} + 0.65 \frac{\text{€}}{\text{MW}}$	[40]
H ₂ Storage specific direct costs	1000 €/kg	[41]
O&M annual costs	5% of IC	[42]
Electricity costs from WF	45 €/MWh	[38]
Electricity costs from PV	80 €/MWh	[38]
Electricity costs from grid	150 €/MWh	
Annual interest rate	5%	[42]
Lifetime	20 years	[42]

4 RESULTS AND DISCUSSION

Starting from the power generation profiles of the 45 MW wind farm (in the reference case, the inclusion of a PV plant is not considered), different values for the PEMEL size and the H₂ storage capacity are considered. In particular, the size of the PEMEL has been designed to use about 10%, 15%, 20%, and 25% of the wind farm rated power, that is a PEMEL rated power input of about 4.5, 6.75, 9.0, and 11.25 MW (the actual power depends on the number of required stacks). Table 6 summarises the yearly energy consumption, the number of stacks, the rated PEMEL input power, and the rated H₂ mass flow production. For a given rated power of the electrolyser, the expected performance of the hydrogen valley is analysed in function of the available hydrogen storage volume.

Table 6. PEMEL unit performance.

WF power percentage	WF energy to PEMEL [GWh/y]	PEMEL stacks [-]	PEMEL power [MW]	H ₂ mass flow [kg/h]
Case 10 %	11.27	676	4.49	76.5
Case 15 %	17.07	1024	6.80	115.73
Case 20 %	22.81	1369	9.09	154.72
Case 25 %	28.01	1681	11.16	189.98

Figure 8(a) shows the annual H₂ production as a function of the available tank volume and the PEMEL size. As can be observed, the hydrogen production linearly increases with the size of the electrolyser due to the consequent rise of the electrical energy provided by the wind farm, while the storage capacity affects the hydrogen production only up to a tank volume of about 2000 m³. In fact, lower storage volumes lead to an H₂ overproduction due to the frequent recourse to electrical energy supplied by the grid during low wind availability periods and the simultaneous occurrence of significant amounts of hydrogen not storable during surplus periods. These aspects will be deeply discussed in the following.

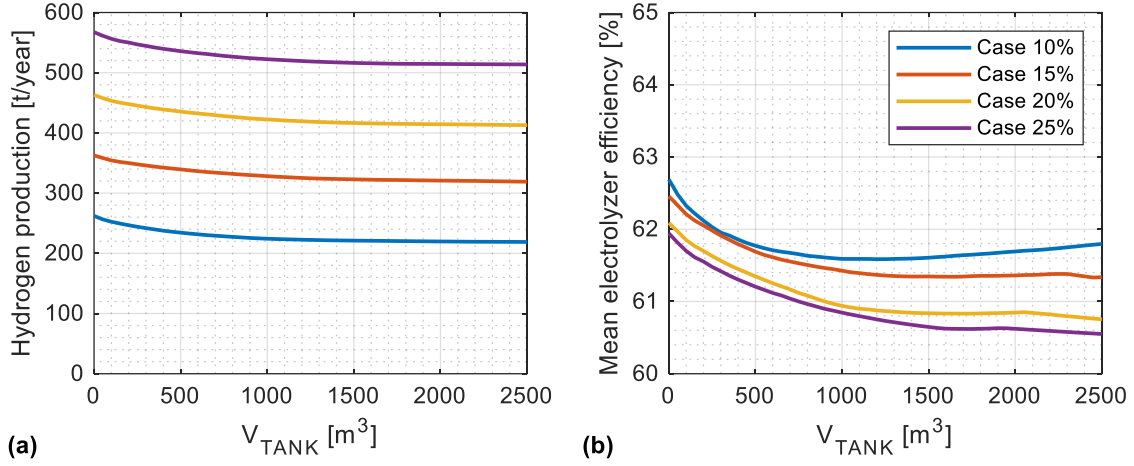


Figure 8- (a) Annual hydrogen production and (b) mean hydrogen generator efficiency as a function of the H₂ tank storage volume and PEMEL size.

Figure 8(b) shows the influence of H₂ storage capacity and electrolyser size on the yearly mean electrolyser efficiency (calculated as the ratio of the annual hydrogen production, in energy primary terms, and the annual electricity consumption). The highest performance is obtained for the smallest tank volumes since the electrolyser very frequently operates at part-load conditions, and therefore with higher conversion efficiencies (as shown by Figure 5). In fact, the lower the storage volume is, the more frequent the storage is completely discharged. In these conditions, it is very frequent that the electrolyser must be kept in operation at part load conditions by using electricity purchased from the grid to cover the not deferrable hydrogen demand (SOFC and refuelling station), which not exceed 45 kg/h. The increase of the PEMEL size, and therefore to the hydrogen production, also reduces the mean electrolyser efficiency. In fact, for the cases “10%” and “15%” the PEMEL operates for longer periods during the year but at a lower average power leading to slightly higher efficiencies.

The annual hydrogen production injected in the NG pipeline as a function of the PEMEL size and tank volume is shown in Figure 9(a). Since the hydrogen demand from the SOFC and refuelling station has the priority, blending is often avoided in the “case 10%”, resulting in a reduction of the average load of the electrolyser, while the amount of hydrogen injected in the NG pipeline for the “case 15%” is more than double than that of the “case 10%”.

On overall, a PEMEL size larger than 6.8 MW is required to achieve a constant blending at 5%_{vol} throughout the year. With the rise of the PEMEL size, a larger tank volume also leads to higher hydrogen injections in the NG pipeline. For instance, for the “case 25%”, a tank volume of about 2000 m³ is required to reach the maximum amount of H₂ injected in the NG pipeline (133 t/year).

Obviously, the larger the PEMEL size the higher the hydrogen surplus is. The amount of the hydrogen surplus neither used for the SOFC unit and the refuelling station nor injected in the NG pipeline is shown in Figure 9(b). Comparison of Figures 8 and 9 demonstrates that a significant share of produced hydrogen is available for other uses, especially for the higher PEMEL sizes. In particular, for a PEMEL size larger than 6.8 MW, this surplus is mainly due to the hydrogen overproduction in comparison with the overall hydrogen demand (30% of the overall production for case 20%, more than 40% for the case 25%). For lower PEMEL sizes the hydrogen surplus depends on the limited storage capacity and the impossibility of storing hydrogen during long windy periods (the hydrogen surplus is less than 10%). Therefore, the presence of other uses for this hydrogen surplus is fundamental to avoid important reductions in the hydrogen production and, consequently, in the economic feasibility of the hydrogen valley.

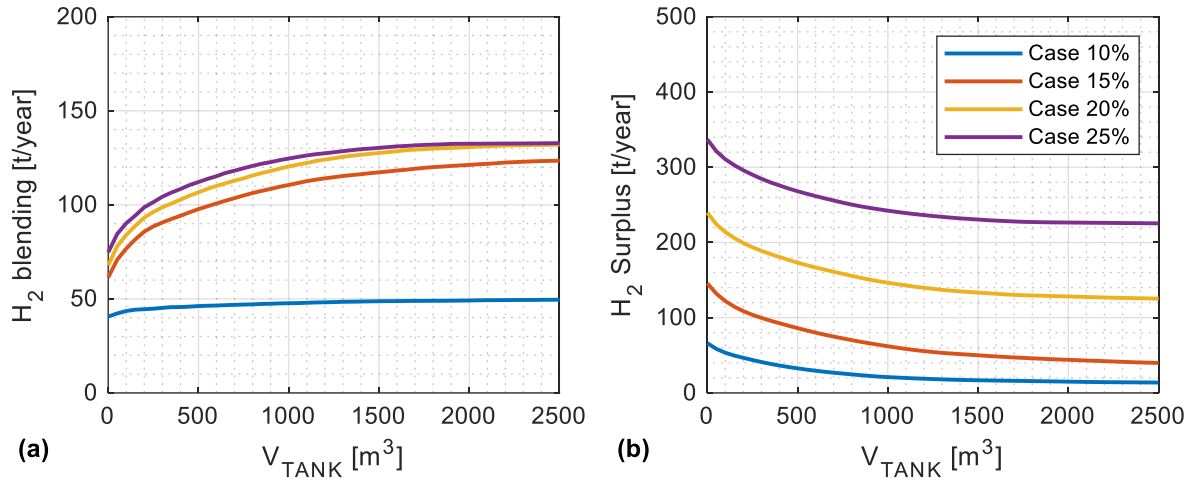


Figure 9. (a) Annual hydrogen production injected in the NG pipeline and (b) annual potential hydrogen production available for the biological methanation as a function of the H_2 tank storage volume and PEMEL size.

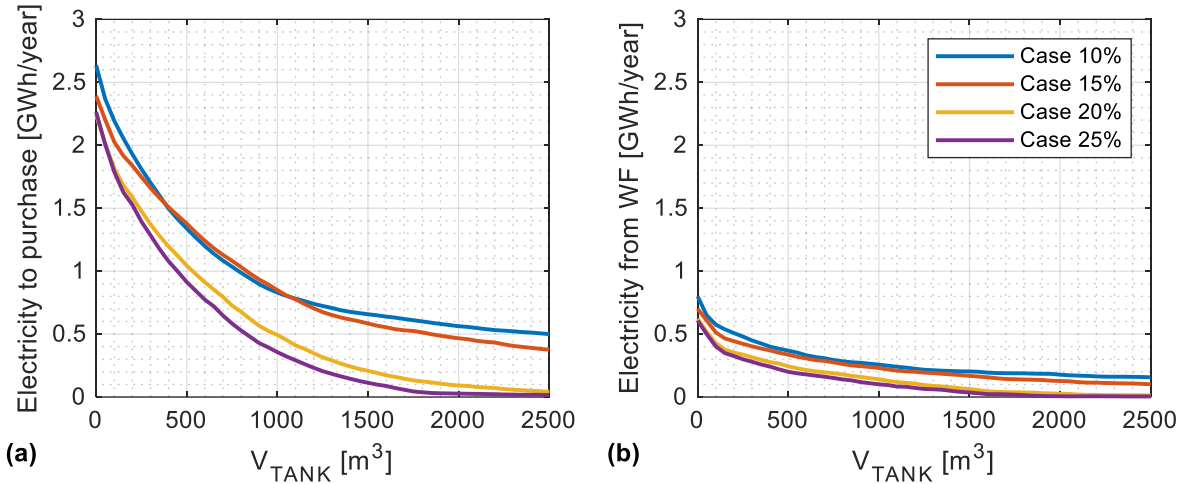


Figure 10 (a) Overall electrical energy to purchase and (b) additional electrical energy available from the wind farm as a function of the H_2 tank storage volume and PEMEL size.

Owing to the limited storage capacity, the purchasing of an extra amount of electrical energy is required to match the hydrogen demand of both the SOFC and refuelling station. Figure 10(a) shows the annual amount of electrical energy supplied by the grid as a function of the H_2 tank volume and PEMEL size. As can be observed, using only the pipeline as a storage system ($V_{TANK}=0$), more than 2 GWh/year should be purchased, corresponding to about 7% of the overall electrical energy used by the PEMEL for a size of 11.16 MW (case 25%) and 20% for a size of 4.49 MW (case 10%). The amount of electricity supplied by the grid strongly decreases with the rise in the tank volume thanks to the growing ability of the hydrogen valley to store the hydrogen surplus, making it available during periods of low hydrogen production. On the other hand, the increase of the PEMEL size reduces the grid electricity demand due to the use of a larger share of the electrical energy produced by the wind farm. However, because the adopted operating strategy gives priority to the supply of the nominal blending demand instead of charging the hydrogen storage, the variation in the state-of-charge of hydrogen storage is quite marginal up to the case 15%. For this reason, the energy supplied by the grid becomes negligible for a V_{TANK} of about 2000 m³ and a PEMEL size larger than 9.09 MW (case 20%),

while much larger tank volumes are required for a PEMEL size smaller than 6.8 MW (case 15%).

Obviously, the use of electrical energy supplied by the grid should be avoided by enabling the use of an additional share of the electrical energy produced by the wind farm. In fact, the hydrogen valley exploits only a given percentage of the overall power output of the WF, even during H₂ deficit periods. The internal electricity consumption can be increased by removing the limit to this power share only during periods of low wind availability. In particular, Figure 10(b) shows the amount of the energy purchased from the grid that could be covered by WF through an extra supply of the WF energy production not dedicated to the hydrogen valley. As can be observed, about 50% of the required electricity can be supplied by the wind farm by increasing the share of WF power output absorbed by the hydrogen generator, even if the complete independency of the hydrogen valley from the electrical grid is achieved only with very large H₂ storage volumes.

4.1 Influence of the energy supply

In the previous section, the performance of a green hydrogen valley using the electrical energy produced by a wind farm were analyzed. In this section, the effect of a partial or complete substitution of the energy supply with a photovoltaic system with the same nominal power (45 MW) is investigated. As case study, the design of the PEMEL adopted for the case 25% (PEMEL power of 11.16 MW) was chosen. The reference case (hereinafter called “100%WF”, that is 100% energy supply from the WF) is compared with other 4 cases: the complete substitution of the WF with a PV system (called 100%PV) and the partial substitution with three different percentages (75%WF-25%PV, 50%WF-50%PV and 25%WF-75%PV). The variation in the annual hydrogen production and mean PEMEL efficiency is shown in Figure 11. It is worth highlighting that although the nominal power of the electrolyser is constant, the lower capacity factor of the PV compared to the WF one results in a reduction of the annual energy consumptions of the hydrogen valley and the consequent decrease in the yearly hydrogen production. On the other hand, the more regular daily power profile of the PV section together with a better daily matching between energy availability and hydrogen request reduces the use of the hydrogen storage section. This results in a lower influence of the hydrogen storage capacity on the hydrogen valley performances. In fact, for the 100% PV case of Figure 11(a), the hydrogen production is essentially constant with the variation of the tank volume (in this case a volume tank of about 150 m³ should be enough to stabilize the hydrogen production, unlike the 100%WF case where a tank volume larger than 1500 m³ is required). Important benefits in terms of mean electricity-to-hydrogen efficiency may arise from the hybridization of the wind energy with the solar energy. In fact, as shown in Figure 11(b), the inclusion of a PV section would increase the mean PEMEL efficiency for all the cases analyzed. The best results are obtained for the case 50%WF-50%PV and 25%WF-75%PV. In these cases, the daily matching between supply and demand of hydrogen is optimized and the highest values of operating hours of the PEMEL are observed (although the hybridization with PV reduces the overall electrical energy available for the hydrogen valley) and its larger use at part-load conditions.

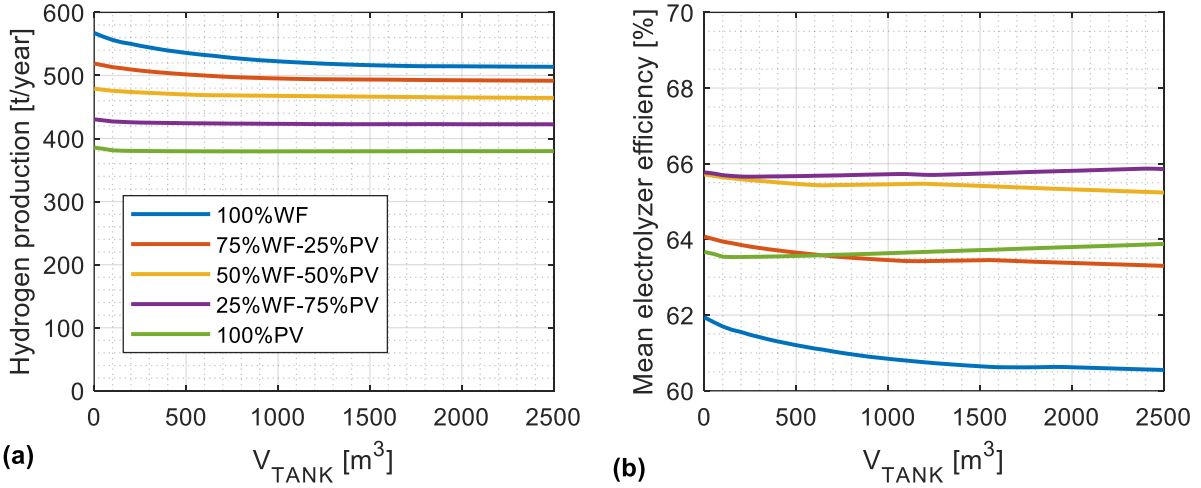


Figure 11 - (a) Annual hydrogen production and (b) mean hydrogen generator efficiency as a function of the H_2 tank storage volume and the energy supply.

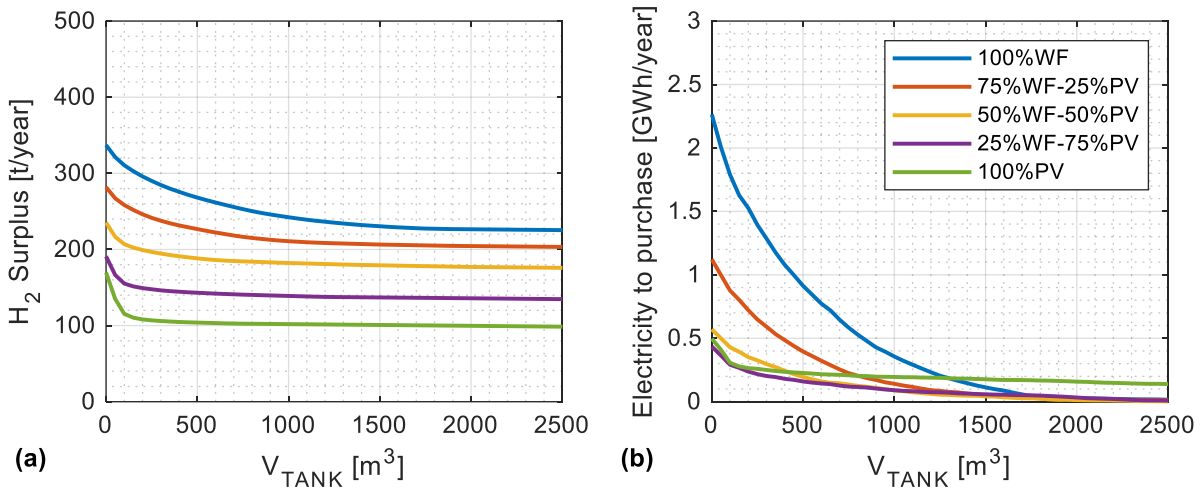


Figure 12 – (a) annual potential hydrogen production available for the biological methanation and (b) Overall electrical energy to purchase as a function of the H_2 tank storage volume and the energy supply.

Due to the different daily power profiles of PV and WF, the mix of the electrical energy supply also reflects on the annual hydrogen surplus and on the electrical energy to be purchased from the grid, as shown in Figure 12. The influence of the energy supply on the percentage of hydrogen injected into the natural gas grid is negligible and therefore the trend observed for the overall hydrogen production directly reflects on the hydrogen surplus available for other uses, such as for a BHM process. In particular, the increase of the PV contribution on the energy supply mix reduces the hydrogen surplus due to the lower capacity factor of this power plant but the more regular daily production profile also reduces the effect of the hydrogen tank volume. An important improvement of the electrical self-sufficiency of the hydrogen system also occurs with the hybridization of the energy supply, as shown in Figure 12(b), especially if the hydrogen storage capacity is limited. This is mainly due to the good matching between the typical daily production profile of the PV plant with the hydrogen SOFC demand, which is concentrated during the sunshine hours.

4.2 Preliminary economic analysis

As mentioned, the feasibility of the proposed hydrogen valley from the economic point of view is investigated by determining the expected levelized cost of hydrogen (LCOH). Figure 13 shows the LCOH as a function of the percentage of the energy absorbed from the WT+PV sections and the percentage of energy supplied by the PV respect to the overall PV+WF energy in case the hydrogen surplus cannot be used. Figure 13 also shows the optimal H₂ tank volume. The latter is the storage capacity reaching the minimum LCOH, representative of the best trade-off between the increase in the investment costs, due to the rise of the storage capacity, and the decrease in the operating costs due to the decrease in the energy purchased from the grid.

As can be observed in Figure 13(a), the LCOH is strongly influenced by the percentage of the energy absorbed from the WT+PV sections (which depends on the PEMEL size), mainly due to the increase of the hydrogen surplus production. On the other hand, the energy supply mix marginally influences the LCOH. In fact, the reduction of the capacity factor of the PV, with the consequent increase of the electricity production costs, is balanced by the reduction of the required tank volumes and the corresponding storage costs. The lowest LCOH values (lower than 7 €/kg) are obtained for a PEMEL able to absorb 10-12% of the overall energy produced by the PV+WF system with a share of PV energy in the range of 20%-50%. In these conditions, the required tank volume is rather low (between 450-750 m³), a constant blending in the natural gas grid is not guaranteed during the year but the hydrogen surplus, which cannot be used and thus curtailed, is minimized. However, the amount of the hydrogen overproduction is not negligible, and negatively impacts on the LCOH. For this reason, the introduction of another end-user, such as a BHM process, is fundamental for the cost-effectiveness of the hydrogen valley. In this regard, Figure 14 shows the minimum achievable LCOH and the corresponding tank volume in case the hydrogen surplus is used by a BHM process. Unlike the previous case, the LCOH is influenced both by the percentage of the energy absorbed from the WF+PV sections and the percentage of energy from PV. In general, the introduction of a PV plant in the energy mix becomes profitable only for high shares of energy consumption from the WF+PV sections (thus, high PEMEL sizes). The best results are obtained for the largest size of PEMEL that allows to use more than 20% of the energy produced by the PV+WF system, and a small share of PV compared to WF (lower than 10%).

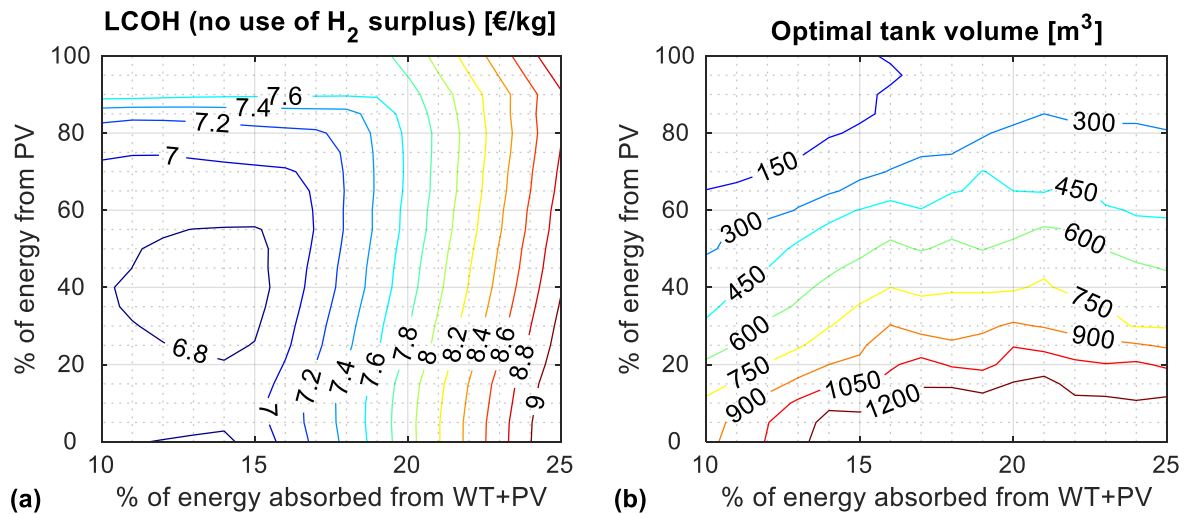


Figure 13. (a) Levelized cost of hydrogen (LCOH) and (b) corresponding optimal tank volume as a function of the PEMEL size and the percentage of the PV in case the hydrogen surplus is curtailed.

The lowest value of the LCOH is about 5 €/kg, which means a reduction of more than 25% compared to that obtained without using the H₂ surplus. As shown in Figure 14(b), with the introduction of the BHM process, the role of the hydrogen storage is less significant and, in several cases, the minimum LCOH is obtained for hydrogen valley configurations not including a dedicated hydrogen storage section. Obviously, this solution is feasible only if a variation in the blending percentage is accepted, otherwise, a volume tank of about 750 m³ is required to guarantee a constant blending at its maximum allowable percentage (5%) with an increase of the minimum LCOH to about 5.2 €/kg. Moreover, in this solution the BHM must be able to receive a variable and irregular amount of hydrogen. However, usually this is not a practical solution, and an additional hydrogen generator and/or hydrogen storage capacity is required for the BHM process.

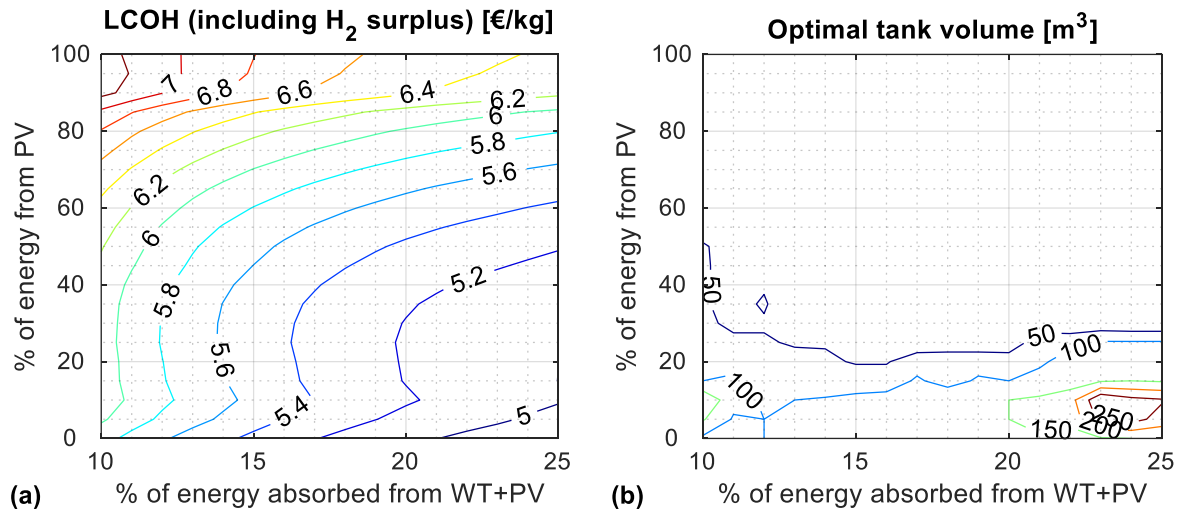


Figure 14 - (a) Levelized cost of hydrogen (LCOH) and (b) corresponding optimal tank volume as a function of the PEMEL size and the percentage of the PV in case the hydrogen surplus is completely used in a BHM process.

4.3 Inclusion of a BHM system

As mentioned, the introduction of a biological methanation plant can be an interesting solution for the hydrogen valley concept.

By considering the “case 25%” with an energy supplier composed by 50% WF-50%PV, a V_{TANK} of 750 m³ is required to guarantee an almost constant injection of hydrogen in the NG grid. In these conditions, the expected LCOH is about 5.2 €/kg but an H₂ surplus of about 180 t/year should be used by the BHM. This overproduction is however intermittent and delivered during specific periods, while a continuous operation of the BHM is required for the thermal and biological stability of the process. Consequently, two different design solutions for the BHM process are investigated: the first solution includes an auxiliary PEMEL while the second includes a smaller auxiliary PEMEL plus an additional storage tank.

The first solution is developed to completely exploit the H₂ surplus, which has a maximum production peaking of 153 kg/h. The bioreactor is therefore designed to operate with this maximum hourly hydrogen feeding and it is integrated with an auxiliary 8.99 MW PEMEL to secure a constant H₂ feed of 153 kg/h. Since the BHM process works with a stoichiometric H₂/CO₂ ratio of 4:1, 1344 t/year of H₂ require about 7335 t/year of CO₂. Therefore, the hydrogen valley is coupled with an equivalent 3 MW_e anaerobic digestion plant with an annual biogas production of about 8.3 million Nm³/year, integrated with a suitable upgrading section. By

assuming a biogas composition of 45%_{vol} of CO₂ and 54%_{vol} of CH₄, the biogas upgrading process can recover about 4.5 million Nm³/year of CH₄. According to [37], with a temperature of 55°C and a pressure of 1 bar the percentage of biomethane achieved in the outlet gas reaches 96%, with the complete conversion of the H₂. Therefore, an additional biomethane production of 3.58 million Nm³/year is expected from the BHM process, with an increase of about 80% in the total amount of CH₄ produced.

In the second case, the bioreactor is designed to operate with a hydrogen capacity of 77 kg/h, half of the maximum hourly surplus value, with a total annual request of 677 t/year. The BHM process is integrated with a H₂ storage tank (capacity of about 77 kg corresponding to an additional volume of about 35 m³), an auxiliary 4.49 MW PEMEL electrolyser, and an equivalent 1.5 MW_e anaerobic digestion plant to produce the required 3668 t/year of CO₂. The operating parameters are the same as the first case, and with 1.79 million Nm³/year of biomethane produced, the total production of CH₄ is increased by about 40%. By including a storage tank, it is possible to use almost 90% of the hydrogen surplus with an increase of the LCOH up to 5.1 €/kg. Increasing the storage capacity by double (from 77 kg to 154 kg), almost 95% of the hydrogen overproduction of the hydrogen valley can be used.

By summing this biomethane production with the annual hydrogen production injected in the NG pipeline (about 125 t/year for the case 25% with a tank volume of 750 m³), the hydrogen valley could cover about 13.5% of the primary energy consumption of the NG pipeline (about 30 Mm³/year) in the first case and 7.6% in the second case.

It is worth noting that if the hydrogen required by the BHM is produced by a dedicated electrolyser without using the hydrogen valley surplus, an expected LCOH of about 5.5 €/kg is determined. Consequently, the inclusion of the BHM process in the hydrogen valley is attractive also from an economic point of view.

5 CONCLUSIONS

A hydrogen valley based on four different applications was analysed in this work. Green hydrogen from a wind farm and/or a PV plant is employed in a stationary application based on SOFC, in a hydrogen refuelling station, for blending on a NG grid, and, optionally, in a BHM process.

Firstly, a techno-economic analysis, based on the wind farm yearly energy production, was carried out for 4 different scenarios based on an electrolyser size equal to 10, 15, 20, and 25% of the wind farm nominal power (45 MW). Depending on the size of the PEMEL and of the storage volume, a hydrogen production between approximately 200 and 600 t/year and a corresponding mean electrolyser efficiency between 60% and 63% were found. The increase in the hydrogen storage reduced the electricity supplied by the grid, which become negligible for tank volumes larger than 2000 m³ and PEMEL sizes bigger than 9 MW, but a hydrogen production surplus of 30%-50% was still observed, which is potentially available for other end-uses, such as a BHM process.

The effect of a partial or complete substitution of the WF energy supply with that of a photovoltaic system with the same nominal power was also investigated. Overall, the substitution of the WF with a PV section leads to a reduction of the hydrogen production but increases the mean PEMEL efficiency and reduces the surplus hydrogen production.

Without including the BHM process, the best compromise, in terms of minimization of the levelized cost of hydrogen, was achieved for a PEMEL that uses about 10-12% of the overall energy production of a PV+WF system with a share of PV energy in the range of 20%-50% and a hydrogen tank volume in the range of 450-750 m³. By considering this hydrogen valley configuration, an expected LCOH of about 6.8 €/kg was obtained. However, the latter solution suffers from a significant hydrogen overproduction compared to the demand of the end-users. Therefore, the hydrogen production cost can be further reduced by introducing another suitable

end-user, such as a BHM process. With reference to a PEMEL with a power input equal to 25% of the power generation section composed by 50% WF-50% PV, the hydrogen surplus can be profitably used in a BHM process with an LCOH of about 5 €/kg, which is lower than the LCOH calculated by supplying the BHM process with the hydrogen produced using a dedicated electrolyser (5.5 €/kg).

ACKNOWLEDGMENT

Giulia Concas gratefully acknowledges Sardinia Regional Government for the financial support for her Ph.D. scholarship (P.O.R. Sardegna F.S.E. Operational Programme of the Autonomous Region of Sardinia, European Social Fund 2014-2020 - Axis III Education and Training, Thematic Goal 10, Specific goal 10.5, Action partnership agreement 10.5.12).

REFERENCES

- [1] Götz M, Lefebvre J, Mörs F, McDaniel Koch A, Graf F, Bajohr S, et al. Renewable Power-to-Gas: A technological and economic review. *Renew Energy* 2016;85:1371–90. <https://doi.org/10.1016/j.renene.2015.07.066>.
- [2] Liu J, Sun W, Harrison GP. The economic and environmental impact of power to hydrogen/power to methane facilities on hybrid power-natural gas energy systems. *Int J Hydrogen Energy* 2020;45:20200–9. <https://doi.org/10.1016/j.ijhydene.2019.11.177>.
- [3] Guandalini G, Robinius M, Grube T, Campanari S, Stolten D. Long-term power-to-gas potential from wind and solar power: A country analysis for Italy. *Int J Hydrogen Energy* 2017;42:13389–406. <https://doi.org/10.1016/j.ijhydene.2017.03.081>.
- [4] Fan G, Yang B, Guo P, Lin S, Farkoush SG, Afshar N. Comprehensive analysis and multi-objective optimization of a power and hydrogen production system based on a combination of flash-binary geothermal and PEM electrolyzer. *Int J Hydrogen Energy* 2021;46:33718–37. <https://doi.org/10.1016/j.ijhydene.2021.07.206>.
- [5] Noussan M, Raimondi PP, Scita R, Hafner M. The role of green and blue hydrogen in the energy transition—A technological and geopolitical perspective. *Sustain* 2021;13:1–26. <https://doi.org/10.3390/su13010298>.
- [6] Rusmanis D, O'Shea R, Wall DM, Murphy JD. Biological hydrogen methanation systems—an overview of design and efficiency. *Bioengineered* 2019;10:604–34. <https://doi.org/10.1080/21655979.2019.1684607>.
- [7] The hydrogen project HyStock › EnergyStock n.d. <https://www.energystock.com/about-energystock/the-hydrogen-project-hystock> (accessed April 13, 2021).
- [8] HyBalance – Green Energy Project Denmark n.d. <http://hybalance.eu/> (accessed April 13, 2021).
- [9] H2FUTURE PROJECT - Startseite n.d. <https://www.h2future-project.eu/> (accessed April 13, 2021).
- [10] REFHYNE – Clean Refinery Hydrogen for Europe n.d. <https://refhyne.eu/> (accessed May 4, 2021).
- [11] The GRHYD demonstration project | Gas | ENGIE n.d. <https://www.engie.com/en/businesses/gas/hydrogen/power-to-gas/the-grhyd-demonstration-project> (accessed May 4, 2021).
- [12] Hidalgo D, Martín-Marroquín JM. Power-to-methane, coupling CO₂ capture with fuel production: An overview. *Renew Sustain Energy Rev* 2020;132. <https://doi.org/10.1016/j.rser.2020.110057>.
- [13] Aguirre-Mendoza AM, Díaz-Mendoza C, Pasqualino J. Renewable energy potential analysis in non-interconnected islands. Case study: Isla Grande, Corales del Rosario Archipelago, Colombia. *Ecol Eng* 2019;130:252–62. <https://doi.org/10.1016/j.ecoleng.2017.08.020>.

- [14] Ozturk M, Dincer I. A comprehensive review on power-to-gas with hydrogen options for cleaner applications. *Int J Hydrogen Energy* 2021;46:31511–22. <https://doi.org/10.1016/j.ijhydene.2021.07.066>.
- [15] Kotowicz J, Jurczyk M, Węcel D. The possibilities of cooperation between a hydrogen generator and a wind farm. *Int J Hydrogen Energy* 2021;46:7047–59. <https://doi.org/10.1016/j.ijhydene.2020.11.246>.
- [16] Cheli L, Guzzo G, Adolfo D, Carcasci C. Steady-state analysis of a natural gas distribution network with hydrogen injection to absorb excess renewable electricity. *Int J Hydrogen Energy* 2021;46:25562–77. <https://doi.org/10.1016/j.ijhydene.2021.05.100>.
- [17] Macedo SF, Peyerl D. Prospects and economic feasibility analysis of wind and solar photovoltaic hybrid systems for hydrogen production and storage: A case study of the Brazilian electric power sector. *Int J Hydrogen Energy* 2022;1–14. <https://doi.org/10.1016/j.ijhydene.2022.01.133>.
- [18] You C, Kwon H, Kim J. Economic, environmental, and social impacts of the hydrogen supply system combining wind power and natural gas. *Int J Hydrogen Energy* 2020;45:24159–73. <https://doi.org/10.1016/j.ijhydene.2020.06.095>.
- [19] Fang R. Life cycle cost assessment of wind power–hydrogen coupled integrated energy system. *Int J Hydrogen Energy* 2019;44:29399–408. <https://doi.org/10.1016/j.ijhydene.2019.03.192>.
- [20] Nastasi B, Lo Basso G. Power-to-Gas integration in the Transition towards Future Urban Energy Systems. *Int J Hydrogen Energy* 2017;42:23933–51. <https://doi.org/10.1016/j.ijhydene.2017.07.149>.
- [21] Walker SB, Van Lanen D, Fowler M, Mukherjee U. Economic analysis with respect to Power-to-Gas energy storage with consideration of various market mechanisms. *Int J Hydrogen Energy* 2016;41:7754–65. <https://doi.org/10.1016/j.ijhydene.2015.12.214>.
- [22] Astiaso Garcia D. Analysis of non-economic barriers for the deployment of hydrogen technologies and infrastructures in European countries. *Int J Hydrogen Energy* 2017;42:6435–47. <https://doi.org/10.1016/j.ijhydene.2017.01.201>.
- [23] Meteonorm Software n.d. <https://meteonorm.com/en/> (accessed May 4, 2021).
- [24] Cocco D, Palomba C, Puddu P. Tecnologie delle energie rinnovabili. 2010.
- [25] Wind turbine Nordex N77 - 1.50 MW n.d. <https://it.wind-turbine-models.com/turbines/76-nordex-n77> (accessed May 4, 2021).
- [26] Duffie J a., Beckman W a., Worek WM. *Solar Engineering of Thermal Processes*, 2nd ed. vol. 116. Hoboken, New Jersey: John Wiley & Sons, Inc., 1994. <https://doi.org/10.1115/1.2930068>.
- [27] SunPower. X-Series: X22-360 DC n.d.
- [28] Emanuele Taibi and Raul Miranda (IRENA), Wouter Vanhoudt, Thomas Winkel J-CL and FB (Hinicio). *Hydrogen From Renewable Power*. 2018.
- [29] Schmidt O, Gambhir A, Staffell I, Hawkes A, Nelson J, Few S. Future cost and performance of water electrolysis : An expert elicitation study. *Int J Hydrogen Energy* 2017;42:30470–92. <https://doi.org/10.1016/j.ijhydene.2017.10.045>.
- [30] Nikiforov A, Christensen E, Petrushina I, Oluf J, J. N. *Advanced Construction Materials for High Temperature Steam PEM Electrolysers*. Electrolysis 2012. <https://doi.org/10.5772/51928>.
- [31] Zhao L, Brouwer J. Dynamic operation and feasibility study of a self-sustainable hydrogen fueling station using renewable energy sources. *Int J Hydrogen Energy* 2015;40:3822–37. <https://doi.org/10.1016/j.ijhydene.2015.01.044>.
- [32] Zhao L, Brouwer J, Samuelsen S. Dynamic analysis of a self-sustainable renewable hydrogen fueling station. *ASME 2014 12th Int Conf Fuel Cell Sci Eng Technol FUELCELL 2014 Collocated with ASME 2014 8th Int Conf Energy Sustain* 2014:1–11.

- <https://doi.org/10.1115/FuelCell2014-6330>.
- [33] Shiva Kumar S, Himabindu V. Hydrogen production by PEM water electrolysis – A review. *Mater Sci Energy Technol* 2019;2:442–54. <https://doi.org/10.1016/j.mset.2019.03.002>.
 - [34] Peng J, Huang J, Wu X long, Xu Y wu, Chen H, Li X. Solid oxide fuel cell (SOFC) performance evaluation, fault diagnosis and health control: A review. *J Power Sources* 2021;505:230058. <https://doi.org/10.1016/J.JPOWSOUR.2021.230058>.
 - [35] Manuel Götz*, Friedemann Mörs, Katharina Bär, Amy McDaniel Koch FG. Comparison of Biological and Catalytic Methanation for Power-to-Gas Applications. 2015.
 - [36] Lecker B, Illi L, Lemmer A, Oechsner H. Biological hydrogen methanation – A review. *Bioresour Technol* 2017;245:1220–8. <https://doi.org/10.1016/j.biortech.2017.08.176>.
 - [37] Voelklein MA, Rusmanis D, Murphy JD. Biological methanation: Strategies for in-situ and ex-situ upgrading in anaerobic digestion. *Appl Energy* 2019;235:1061–71. <https://doi.org/10.1016/j.apenergy.2018.11.006>.
 - [38] IRENA. Renewable Power Generation Costs in 2020. Abu Dhabi.: 2020.
 - [39] IRENA. Green Hydrogen Cost Reduction: Scaling up Electrolysers to Meet the 1.5°C Climate Goal. 2020.
 - [40] DOE Hydrogen and Fuel Cells Program. 2020. https://doi.org/https://www.hydrogen.energy.gov/annual_progress19.html.
 - [41] Parra D, Valverde L, Pino FJ, Patel MK. A review on the role, cost and value of hydrogen energy systems for deep decarbonisation. *Renew Sustain Energy Rev* 2019;101:279–94. <https://doi.org/10.1016/j.rser.2018.11.010>.
 - [42] Serra F, Lucariello M, Petrollese M, Cau G. Optimal integration of hydrogen-based energy storage systems in photovoltaic microgrids: A techno-economic assessment. *Energies* 2020;13. <https://doi.org/10.3390/en13164149>.